

AD-A052 586

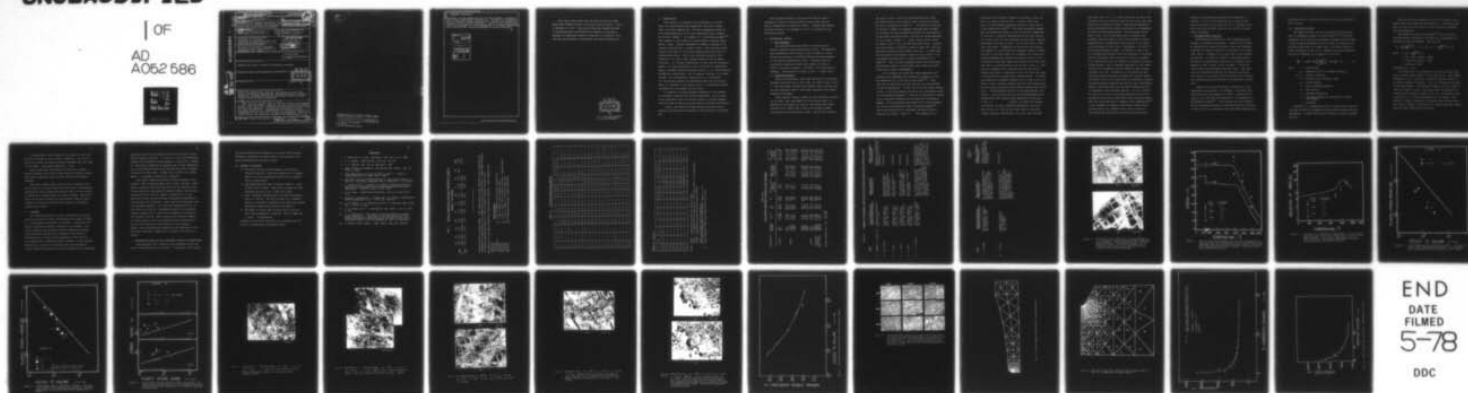
CINCINNATI UNIV OHIO DEPT OF MATERIALS SCIENCE AND --ETC F/G 11/6
MICROSTRUCTURAL EFFECTS AND FATIGUE LIFE PREDICTIONS OF NOTCHED--ETC(U)
FEB 78 S D ANTOLOVICH

UNCLASSIFIED

AFOSR-TR-78-0536

NL

1 OF
AD
A052 586



END
DATE
FILMED
5-78
DDC



MICROCOPY RESOLUTION TEST CHART
NATIONAL BUREAU OF STANDARDS-1963-A

1. REPORT DOCUMENTATION PAGE		READ INSTRUCTIONS BEFORE COMPLETING FORM	
2. GOVT ACCESSION NO.	3. RECIPIENT'S CATALOG NUMBER		
4. TITLE (and Subtitle)		5. TYPE OF REPORT & PERIOD COVERED	
6. AUTHOR(s)		7. PERFORMING ORG. REPORT NUMBER	
8. CONTRACT OR GRANT NUMBER(s)		9. PROGRAM ELEMENT, PROJECT, TASK AREA & WORK UNIT NUMBERS	
10. CONTROLLING OFFICE NAME AND ADDRESS		11. REPORT DATE	
12. MONITORING AGENCY NAME & ADDRESS (if different from Controlling Office)		13. NUMBER OF PAGES	
14. DISTRIBUTION STATEMENT (of this Report)		15. SECURITY CLASS. (of this report)	
16. DISTRIBUTION STATEMENT (of the abstract entered in Block 20, if different from Report)		17. SUPPLEMENTARY NOTES	
18. KEY WORDS (Continue on reverse side if necessary and identify by block number)		19. ABSTRACT (Continue on reverse side if necessary and identify by block number)	

DD FORM 1 JAN 73 1473

EDITION OF 1 NOV 65 IS OBSOLETE

405-382
SECURITY CLASSIFICATION OF THIS PAGE (When Data Entered)

AD A 052586

AD No. 1
DDC FILE COPY

Approved for public release; distribution unlimited

DDC

APR 13 1978

D

Nickel Base Superalloys, René 80, High temperature low cycle fatigue, dislocation substructure, optical microscopy, scanning microscopy, transmission electron microscopy, notch low cycle fatigue, creep fatigue interactions

The low cycle fatigue (LCF) of René 80 has been investigated at 1400, 1600 and 1800°F. Emphasis has been placed on the 1800°F studies using smooth bar (continuous cycling and 90 sec hold time) and notch LCF specimens. The detailed transmission electron microscopy shows that at 1600 & 1800°F the dislocation debris is independent of test rate over two orders of magnitude. The test results can not be explained in terms of the conventional

AIR FORCE OFFICE OF SCIENTIFIC RESEARCH (AFSC)
 NOTICE OF TRANSMITTAL TO DDC
 This technical report has been reviewed and is
 approved for public release IAW AFR 190-12 (7b).
 Distribution is unlimited.
 A. D. BLOSE
 Technical Information Officer

RECEIVED
 APR 13 1978
 DDC

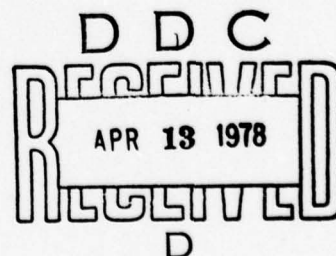
98220 A DA
 DDC LIFE 0052

20. ABSTRACT (continued)

approaches to high temperature LCF for which damage is assumed to result from creep/fatigue interactions. Instead, it is suggested that the important damage mechanism is an interaction between the deformation mode and the environment. Based on that understanding a model is developed for crack propagation at elevated temperatures and a similar model is being developed for crack initiation.

ACCESSION 1W	
RTS	White Section <input checked="" type="checkbox"/>
DOC	Buff Section <input type="checkbox"/>
UNANNOUNCED	<input type="checkbox"/>
JUSTIFICATION.....	
BY.....	
DISTRIBUTION/AVAILABILITY CODES	
Dist.	AVAIL. and/or SPECIAL
A	

This report covers work that has been carried out under AFOSR grant #AFOSR-76-2952 for the grant period January 1, 1977 to December 31, 1977. This project has been renewed and work is continuing under the direction of Stephen D. Antolovich, Professor of Materials Science, University of Cincinnati. This work has been prepared in accordance with AFOSR instructions.



Approved for public release;
distribution unlimited.

I. INTRODUCTION

This project is concerned with development of a sound basis for understanding high temperature low cycle fatigue (LCF) in Ni base superalloys. The most fundamental aspect of that understanding has to do with ascertaining what is meant by the term "damage." For example, it is generally assumed⁽¹⁻³⁾ that "damage" is the result of various forms of plastic deformation, either athermal deformation (commonly referred to as "plastic" deformation) or creep or both. Laws have been formulated on the basis of intuitively appealing yet physically unsubstantiated ideas. Thus a very important aspect of this study has to do with a very careful evaluation of the possibilities: (1) "plastic" deformation in the form of dislocation debris; (2) creep deformation, also in the form of dislocation debris (although possibly different from (1)); (3) creep/"plastic" deformation interactions, this is commonly referred to as creep/fatigue; (4) environmental interactions (e.g. oxidation); (5) interactions between the deformation mode and the environment; (6) formation of new phases; and (7) interactions between new phases the environment and slip mode.

In addition to studying damage accumulation, the effects of structural stability are being investigated. This is especially important since long service times at elevated temperatures and high stresses can cause radical structural alterations.

Finally, the results of these studies are being used to develop life prediction techniques in both smooth bar and notch LCF.

The principal material is cast and HIP René 80 since it represents a typical current generation cast blade material used at temperatures in excess of 1800°F. Progress made during the period January 1 to December 31, 1977, is outlined in the following sections.

II. EXPERIMENTAL RESULTS

A. Heat Treatment

All specimens have been HIPed to reduce porosity, improve properties and minimize data scatter. The specimens were subsequently heat-treated to give a duplex γ' microstructure consisting of cuboidal precipitates approximately 1μ and spheres approximately 0.05μ . The heat-treat was essentially commercial except final ageing was done at 1400°F to maximize strength. See Table I for heat-treating schedule. The structure is shown in Fig. 1 in dark field.

B. Mechanical Testing

After heat-treatment, tests were carried out to evaluate strength and ductility at 1400, 1600, and 1800°F, Figs. 2 and 3. Note the higher strength and somewhat lower ductility for the heat-treatment used in this study compared to the normal commercial treatment.

After tensile testing, smooth bar LCF tests were carried out at 1400, 1600, and 1800°F at low and high rates. In addition to the continuous cycling, LCF studies have been carried out at 1800°F with a hold of 90 seconds at peak strain and low and high strain rates. The LCF test results

are shown in Figs. 4 and 5 as Coffin-Manson plots (data for 1400°F tests is not extensive and is thus not plotted). The data is tabulated in Table II. In addition to cycling to failure, a number of companion specimens were unloaded at the point of crack initiation and used for investigation of the crack initiation sites. The data for these specimens is also listed in Table II. Cyclic stress strain curves are shown in Fig. 6 for the 1600 and 1800°F tests. Finally, the total energy to failure is shown in Table III. This was obtained by measuring the average loop area. In some cases the loop width was extremely narrow and an estimate of the loop energy was made using a formula developed by the author⁽⁴⁾. Note the good agreement between the calculated and measured values of total energy where there was sufficient data to make a measurement.

It is customary to assume that high temperature LCF properties are degraded with decreasing frequency or with the imposition of a hold time at peak load⁽¹⁻³⁾. Note that this is definitely not the case for the alloy studied in this investigation. In fact, as can be seen quite clearly in Fig. 5, the life actually *decreases* with increasing strain rate (increasing frequency). This can be understood in terms of an interaction between the slip mode and environmental damage. It has previously been shown that at high stresses the rate of environmental attack is greatly enhanced⁽⁵⁾. Now as the strain rate is increased, the peak stress is generally increased, Table II. The combination of

accelerated environmental damage and increased stress can lead to a greatly reduced life. A similar effect was seen in stress exposed specimens tested at a high rate to a more pronounced extent⁽⁶⁾. The above hypothesis assumes that the dislocation debris in the lattice was independent of test rate. Extensive TEM examination has been carried out on this alloy for the continuous cycling case. Typical micrographs are shown in Figs. 7-10 for LCF tests at 1400, 1600, and 1800°F. Regardless of strain rate the dislocation density was non-uniform for specimens tested at 1400°F and even at low rates there was a tendency for linear dislocation segments and extensive faulting as seen in Fig. 7. It should be noted that there were regions where there were very few or no dislocations as can be seen in Fig. 8. Note also the residual strain contrast from the very fine γ' between the larger γ' particles and the fact that the large γ' particles have retained their cuboidal shape. At 1600°F the situation is somewhat changed as can be seen in Fig. 9. There is still residual contrast from the fine precipitates but the larger precipitates have become somewhat more irregular. The dislocations tend to be localized between the large γ' . The dislocations were also inhomogeneously distributed with many regions being identical to that seen in Fig. 1a. Finally, at 1800°F the dislocation density is again completely homogeneous as can be seen in Fig. 10. The low rate test tends to have more regular arrays of dislocations, Fig. 10a, than the high

rate test, Fig. 10b. It is also clear that the small precipitates have been dissolved and that the larger ones have become more irregular in shape. The previous hypothesis about environmental/slip mode interactions is strengthened by these last photomicrographs. The dislocation debris shown in Fig. 10b for the high rates is probably more damaging than that shown in 10a so the concept of severe degradation by "creep/fatigue interactions" is not physically verified for this alloy. Furthermore, the alloy is not microstructurally stable: it changes in such a way as to become more ductile since the structure is coarsened and the dislocation mean free path is greatly increased. In no cases did we see any evidence of boundary cavitation during fatigue. This is probably explained by the irregularity of the boundaries and the numerous grain boundary carbides, Fig. 10b. In addition to the smooth bar LCF, notch LCF studies have been initiated and several results are shown in Fig. 11 for high rates and continuous cycling. The microstructural aspects have not yet been investigated. However, some analytical work has been underway and this is discussed in the following section. It is of interest to note that in order to get good predictions of the experimental data using a theory that gives excellent agreement for other materials at somewhat lower temperatures⁽⁷⁾ it was necessary to assume a theoretical stress concentration factor of 2 instead of the correct value of 3. The reasons for this may be related to microstructural

stability and detailed microstructural examination is underway. It will be recalled that in the most recent renewal proposal, it was shown that the γ' changes at the notch root were different than was the case for uniaxial tensile specimens.

C. Microstructural Stability

Microstructural stability at high temperatures and stresses is probably not possible. Stress has the effect of exponentially enhancing diffusion rates and although a structure is *thermally* stable it is unlikely to be stable under stress. Evidence of this was shown in the preceding section. An effort to develop a temperature/stress envelope of microstructural stability is underway and an example of this is shown in Fig. 12 where γ' plates on $\{100\}$ planes have developed from small cubes. The properties of coarsened structures are obviously different than those of the as-heat treated structure and in making life predictions and correlations this knowledge is essential.

Another form of microstructural instability is the appearance of new phases. For example, it has been indicated that with long exposure at 1800°F a combination of $M_{23}C_6/\gamma'$ will form and this combination is susceptible to environmental damage⁽⁸⁾. This question has been investigated by microprobe analysis using back-scattered electrons. To date there is no indication that such phase changes occur.

This may be due to insufficient precision and the technique is being refined.

III. ANALYTICAL STUDIES

The author has been actively involved with the development of fundamental models for LCF and FCP^(4,9-12). With the indication of an interaction between environment and slip mode, a model is being developed for FCP in terms of cracking of an oxidized layer ahead of a sharp crack. The model predicts a direct dependence of FCP on ΔK , frequency and other parameters and may be expressed by an equation of the form:

$$\frac{da}{dn} = C_1 \sqrt{D_0} \exp \left(\frac{C_2 \bar{K}^{4n}}{\sigma_{ys}^{2n} RT} \right) \cdot \exp - \frac{Q}{RT} \cdot \frac{1}{v} \quad \dots (1)$$

where a = crack length

D_0 = frequency factor in diffusion equation

C_1, C_2 = material constants

\bar{K} = average stress intensity range

σ_{ys} = yield strength

n = strain hardening exponent

R = gas constant

T = absolute temperature

Q = activation energy for diffusion (of oxygen, for example)

v = frequency

Equation (1) is appealing since it contains major materials and test variables and appears to qualitatively predict correct dependences. A model using similar concepts is being developed for LCF.

Work has also been underway to refine and extend a finite element model for predicting notch behavior. Preliminary analyses to verify the stress state in the notched bar specimens have been completed.

The closed form solution of Neuber⁽¹³⁾ for an infinite circumferentially notched bar was used as an approximation to the actual notch bar geometry. The equation:

$$K_t = \frac{1}{N} \left[\frac{a}{\rho} \sqrt{\frac{a}{\rho} + 1} + (.5 + \nu) \frac{a}{\rho} + (1 + \nu) \left(\sqrt{\frac{a}{\rho} + 1} + 1 \right) \right]$$

where: $N = \frac{a}{\rho} + 2\nu \sqrt{\frac{a}{\rho} + 1} + 2$

a = min. sect. radius = .0885"

ρ = notch root radius = .009"

ν = poisson's ratio

determines $K_t = 3.29$.

As a check and as a precursor to an elastic-plastic solution, a finite element model of the notch was run. The element breakdown in Fig. 13 was used to model one quarter section of the doubly symmetric structure. Fig. 14 illustrates the detail in the notch region. (The smallest element is of the order of .002-.003 inches in size.) The axial stress distribution obtained from this model is shown in Fig. 15. This model yields a value of $K_t \approx 3.5$ when extrapolated to the surface. The scatter in element stresses for distances away from the notch less than .02 inches is indicative of insufficient model refinement and makes extrapolation difficult.

A refined model, with elements of the order of .001 inch was run to attempt to gain a better comparison. Fig. 16 is a plot of the axial and maximum principal stresses near the notch in this model. This model predicts $K_t \approx 3.30$.

Thus a sufficient verification of the finite element method and Neuber solutions has been shown for elastic loading. This permits confident entry into the follow-on non-elastic analyses.

The finite element model (with the fine breakdown) will now be used in an elastic-plastic solution mode to analytically determine the notch stresses and strains when the local region is subjected to stresses above the yield strength. This solution will be used to assess the test specimen behavior and to attempt to correlate microstructural changes to calculated stress/strain fields.

IV. PERSONNEL

All research personnel who have contributed to this program and the nature of their contributions are listed in Table IV. The principal Investigator is Stephen D. Antolovich, Professor of Materials Science, University of Cincinnati. His recent interests have included elevated temperature fatigue life predictions (notched and un-notched), the effects of microstructure on fatigue crack propagation (both high and low temperatures), improved fracture toughness in high strength materials as a result of controlled phase transformations, stress corrosion cracking and corrosion fatigue in high strength

materials and low cycle fatigue and corrosion fatigue of biomedical implant materials. In addition to the high temperature fatigue work described in this proposal a recent Ph.D. student, Dr. Paul Bania, completed his dissertation on high temperature LCF in the titanium alloy Ti-5Al-5Sn-2Mo-2Zr-0.25Si at Wright-Patterson Air Force Base. Another Ph.D. student, Mr. Shahid Bashir, is currently studying LCF in René 95.

Four thesis students have been actively working on this program. They are Messrs. Domas, Baur, Aizaz, and Rosa. Both Messrs. Domas and Baur hold positions with the Materials and Process Technology Laboratory of General Electric and are pursuing their Ph.D. and M.S. degrees, respectively, in the Materials Science and Metallurgical Engineering Department of the University of Cincinnati. Amer Aizaz and Ed Rosa are full-time graduate students. Mr. Aizaz has completed his M.S. in the field of LCF and FCP in maraging steels and is presently working towards a Ph.D. While four students are assigned to this project, only Mr. Aizaz receives full financial support. Mr. Rosa receives 75% of his stipend from the University as part of the University's contribution to this research. Messrs. Baur and Domas, even though full-time employees of G.E., are given occasional release time to pursue their thesis research.

V. INTERACTIONS WITH AIR FORCE SPONSORED PRINCIPAL INVESTIGATORS

During October 1977 a meeting of the Superalloy Group was held at the University of Cincinnati. In addition, close contact

has been maintained with Professor R. Pelloux of MIT through exchange of proposals, progress reports and occasional telephone conferences and one visit to MIT.

VI. REPORTS IN PROGRESS

- 1) The Effect of Prior Stress Exposure on Low Cycle Fatigue of René 80. With Paul Domas and J.L. Strudel. Paper is out for preliminary review prior to submission for publication.
- 2) High Temperature Low Cycle Fatigue of René 77. With Ed Rosa and A. Pineau. First draft of paper has been completed and sent to Dr. Pineau for review.
- 3) Misfit Parameter Determination in Ni Base Superalloys. With J.L. Strudel. The work on René 80 is complete. However, we decided to generalize the paper and include additional alloys such as René 95 and René 77.
- 4) The Effect of Strain Rate and Hold Time on the Low Cycle Fatigue Behavior of René 80. With P. Domas and A. Aizaz. In preparation.

Preprints of the first two papers are available and will be sent to AFOSR after preliminary review.

References

1. A. Abel and R. K. Ham: Acta Met., 1966, Vol. 14, p. 1489.
2. S. S. Manson: ASTM STP 490, 1973, pp. 744-782.
3. L. F. Coffin, Proc. ICM II, ASM 1976 p. 866.
4. Ashok Saxena and Stephen D. Antolovich: Met. Trans., Vol. 6A, 1975, p. 1809.
5. High Temperature Low Cycle Fatigue of René 77. Paper in preparation with A. Pineau and E. Rosa.
6. The Effect of Prior Stress Exposure on Low Cycle Fatigue of René 80. Manuscript completed with P. Domas and J. L. Strudel.
7. J. Bartos and S. D. Antolovich: "Effect of Microstructure on the Fatigue Crack Growth of a Powder Metallurgy Nickel Base Superalloy." Volume 2, ICF4, p. 995, 1977.
8. W. H. Chang: Superalloys-Processing, section V, MCIC-72-10, 1972.
9. Stephen D. Antolovich, A. Saxena and G. R. Chanani: Engineering Fracture Mechanics, vol. 7, 1975, pp. 649-652.
10. G. R. Chanani, S. D. Antolovich and W. W. Gerberich: Met. Trans. Vol. 3, 1972, p. 2661.
11. G. R. Chanani and S. D. Antolovich: Met. Trans., vol. 5, 1974, p. 217.
12. S. D. Antolovich: "The Effect of Microstructure on Fatigue Crack Propagation." Presented at the 40th Meeting of the AGARD Structures and Materials Panel, Brussels, April, 1975. Published January, 1976, Proceedings No. 185, pp. DS4-DS14.
13. H. Neuber: Trans. ASME, J. Appl. Mech., 1961, pp. 544-550.

TABLE I NOMINAL COMPOSITION AND HEAT TREATMENT OF RENÉ 80

	<u>Weight % of Element</u>									
	<u>Al</u>	<u>Ti</u>	<u>Cr</u>	<u>Mo</u>	<u>W</u>	<u>C</u>	<u>Co</u>	<u>B</u>	<u>Zr</u>	<u>Ni</u>
<u>Min.</u>	2.80	4.80	13.7	3.70	3.70	0.15	9.0	0.010	0.02	Bal
**	(3.00)	(4.87)	(13.80)	(4.06)	(3.90)	(0.15)	(9.60)	(0.014)	(0.02)	(2.27)
<u>Max.</u>	3.20	5.20	14.3	4.30	4.30	0.19	10.0	0.020	0.04	

Nv₃*
2.32
(2.27)

*Average electron vacancy number. This number must be kept less than 2.50 to prevent the appearance of sigma phase in the temperature regime of 1200-1700°F. Sigma phase formation is stress enhanced and leads to a loss of rupture strength and ductility.

**Composition of specimens supplied by MISCO Vendor Analysis. Other elements are:

<u>Heat Treatment</u>	
Mn:	<0.10
Si:	<0.10
P:	<0.10
S:	<0.00 22
cb:	<0.10
Ta:	<0.10
Cu:	<0.10
V:	<0.10
Hf:	<0.10
Mg:	<0.10

- 2 hrs. @ 2200°F and He quench (solutinize)
- 4 hrs. @ 2000°F and He quench (age)
- 4 hrs. @ 1925 ~ FC to 1200°F in 20 min. (coating cycle)
- 16 hrs. @ 1400°F - AC to RT (final age)

This treatment develops a duplex structure.

TABLE II LCT TEST RESULTS FOR RENE 80

Spec. No.	Test type	Temp. (°F)	$\Delta \epsilon_p^a$	$\Delta \epsilon_e^a$	Cycles $\times 10^{-6}$	End stress (ksi)		N_i	N_f	Frequency $H_z \times 60$	Strain rate (%/min.)	Comments
						Max.	Min.					
16IV-7	CCF	1400	0.0064	0.7	615	100.1	-74.4	1243	1799	5	7	failed
16IV-8	"	"	0.0259	0.715	1100	94.9	-71.1	1755	2234	50	71.5	failed
16IV-9	"	1600	0.024	0.620	437	92	-46.8	732	1645	5	6.2	failed
16IV-10	"	"	0.017	0.782	550	93	-93.0	710	1516	50	78.2	failed
16IV-11	"	"	0.020	0.500	1500	101	-8.5	-	2980	45	45.0	failed
16IV-12	"	"	0.062	0.670	350	103.7	-34.6	-	710	21.6	29	failed
16IV-13	"	"	0.044	0.72	250	115.2	-69.2	-	530	21.6	31	failed
16IV-14	"	1800	0.036	0.444	760	61.3	-31.9	1561	3232	5	4.4	failed
16IV-15	"	"	0.053	0.586	1000	58.5	-48.6	1254	1645	50	58.6	failed
18IV-1	"	"	0.040	0.300	2344	31.1	-27.1	4772	5445	0.69	0.419	failed
18IV-2	"	"	0.184	0.532	68	36.6	-33.8	523	877	0.434	0.462	failed
18IV-3	"	"	0.192	0.552	422	35.5	-35.5	473	-	0.434	0.462	removed @ 503
18IV-4	"	"	0.040	0.468	990	49.4	-40.8	2119	2511	56.70	53.1	failed
18IV-5	"	"	0.040	0.476	775	50.3	-33.3	1525*	-	56.70	54	removed @ 1810
18IV-6	"	"	0.140	0.624	400	54.3	-48.1	753	931	43.4	54.2	failed
18IV-7	"	"	0.136	0.624	440	54.3	-51.7	752*	-	43.4	54.2	removed @ 848
18IV-8	"	"	0.034	0.332	1202	24.4	-30.0	1417	1620	0.70	0.46	failed
18IV-9	H.T. LCF	"	0.372	0.476	727	26.4	-62.2	835	1457	56.7	54.0	failed
18IV-10	"	"	0.196	0.532	257	32.8	-39.0	526	573	0.434	0.462	failed
18IV-11	"	"	0.212	0.532	294	34.0	-38	331	-	0.434	0.462	removed
18IV-12	"	"	0.230	0.624	283	47.4	-64.8	378	482	43.4	54	failed

TABLE II (Contd.)

Spec. No.	Test type	Temp. (°F)	$A\epsilon_p$	$A\epsilon_t$	Cycles	$E \times 10^{-6}$	End Stress (ksi)		N_i	N_f	Frequency $H_3 \times 60$	Strain rate (1/min.)	Comments
							Max.	Min.					
18NIV-3	CCLCF	1800°F	- - -	- - -	- - -	- - -	33.25	1.75	- - -	243.0	56.7	- - -	run out
18NIV-4	"	"	- - -	- - -	- - -	- - -	39.1	2.1	27,321	28,462	56.7	- - -	failed
18NIV-8	"	"	- - -	- - -	- - -	- - -	39.1	2.1	38,129	- - -	56.7	- - -	removed
18NIV-5	"	"	- - -	- - -	- - -	- - -	66	3.5	465	790	43.4	- - -	failed
18NIV-2	"	"	- - -	- - -	- - -	- - -	66	3.5	549	- - -	43.4	- - -	removed
18NIV-7	"	"	- - -	- - -	- - -	- - -	47.5	2.5	3807	6562	43.4	- - -	failed
18NIV-1	"	"	- - -	- - -	- - -	- - -	58.1	3.1	1020	1808	43.4	- - -	failed
18NIV-9	"	"	- - -	- - -	- - -	- - -	58.1	3.1	1378	- - -	43.4	- - -	removed

Code: CCLCF : Continuous cycling low cycle fatigue.

HTLCF : 90 second hold at peak strain. The rates refer to the ramp rate.

CCNLCF : Continuous cycling notch low cycle fatigue.

* Crack initiated outside extensometer.

All notch testing done in load control mode, $A = 0.9$

** Step loaded at 3200 cycles from 36 ksi to 37 ksi.

TABLE III
LOOP ENERGY ANALYSIS OF RENÉ 80 LCF SPECIMENS

Temperature	Specimen Number	$\Delta \epsilon_p$ (%)	$\Delta \sigma$ ksi	N_f	ΔW Avg. Loop Energy in-lb/in ³	ΔW_t , Total loop energy in-lb/in ³	$n' = .214$ $*\Delta W_t$ calculated in-lb/in ³
1400°F	LL7	0.0064	174.5	1799	9.2		16.5 x 10 ³
	LL8	0.0259	166.0	2234	35.4		79.1 x 10 ³
1600°F	LL9	0.024	138.8	1645	24.6	40.6 x 10 ³	45.1 x 10 ³
	LL10	0.017	186.0	1516	11.4	34.6 x 10 ³	39.5 x 10 ³
	16LV3	0.02	109.5	2980	17.7	52.9 x 10 ³	53.7 x 10 ³
	16LV7	0.06	138.3	710	61.7	43.8 x 10 ³	48.5 x 10 ³
	16LV8	0.044	184.4	530	61.7	32.7 x 10 ³	35.4 x 10 ³ ($n' = .295$)
1800°F	18LV2	0.04	58.2	5445	17.8	96.8 x 10 ³	104.4 x 10 ³
	18LV3	0.04	90.2	2511	27.2	68.4 x 10 ³	74.6 x 10 ³
	18LV5	0.184	70.4	877	91.6	80.2 x 10 ³	93.6 x 10 ³
	18LV7	0.14	102.4	931	102.4	95.4 x 10 ³	110 x 10 ³
	LL11	0.036	93.2	3232	26.6	85.6 x 10 ³	89.3 x 10 ³
	LL12	0.053	107.1	1645	42.2	69.3 x 10 ³	79.9 x 10 ³
	18HLV1	0.084	55.3	1620	33.8	54.7 x 10 ³	62.0 x 10 ³
	18HLV4	0.104	88.6	1457	84.2	122.6 x 10 ³	110.6 x 10 ³
	18HLV5	0.196	71.8	573	108.6	62.2 x 10 ³	66.4 x 10 ³
	18HLV8	0.23	102.2	483	180.4	87.1 x 10 ³	93.5 x 10 ³ ($n' = .214$)
	90 second hold at peak strain						

*Using formula $\Delta W_t = N_f \cdot \frac{\Delta \sigma \cdot \Delta \epsilon_p}{1 + n'}$

SUMMARY OF PERSONNEL ASSOCIATED WITH PROJECT DURING FIRST RENEWAL PERIOD

TABLE IV

<u>Name</u>	<u>Title and Dates Of Project Participation</u>	<u>Topic or Area of Responsibility</u>	<u>Status in Project Participation</u>
1. Stephen D. Antolovich	Principal Investigator Jan. 1, 1976 -		Professor of Materials Science, University of Cincinnati
2. Paul Domas	Graduate Research Assistant Pursuing Ph.D. Jan. 1, 1976 -	Elevated Temperature Notch Fatigue Life Predictions Including Hold Time Effects	Continuing
3. R. Baur	Graduate Research Assistant Pursuing M.S. Jan. 1, 1976 -	Hold Time Effects In Smooth Bar LCF	Continuing
4. A. Aizaz	Graduate Research Assistant Pursuing Ph.D. Jan. 1, 1976 -	The Relationship Between LCF and FCP at High Temperatures in René 80	Continuing
5. E. Rosa	Graduate Research Assistant Pursuing M.S. Sept. 27, 1976 -	Metallography of René 77 LCF Specimens	Continuing
6. J. L. Strudel	Group Leader at Centre des Matériaux, France. Jan.-June 30, 1976	Dr. Strudel assisted with much of the TEM and SEM work that was done in the initial phase of this pro- ject. He was very helpful in pointing out appropriate experimental approaches for the TEM work.	Project results are being discussed on a continuing basis with Dr. Strudel. He gave a TEM course at U.C. in August, 1977. All aspects of the course were supported by U.C.

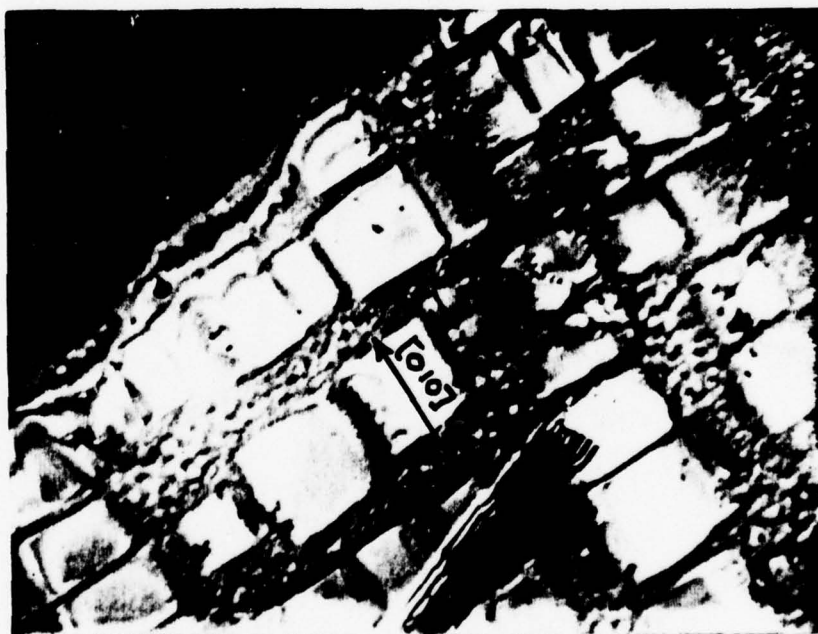
TABLE IV
Page 2

<u>Name</u>	<u>Title and Dates of Project Participation</u>	<u>Topic or Area of Responsibility</u>	<u>Status in Project Participation</u>
7. A. Pineau	Group Leader at Centre des Materiaux, France Jan.1-Sept.30, 1976	Dr. Pineau generously made his fatigue laboratory available to carry out a study of René 77 at 1700°F and participated in analysis of results.	Project results are being discussed on a continuing basis with Dr. Pineau.
8. A. Coles	Manager, Materials Criteria Section, G.E. Evendale Jan. 1, 1976 -	Mr. Coles has acted in the capacity of an advisor. His participation has been greatly appreciated because of his outstanding knowledge of high temperature fatigue on Ni base superalloys.	Continuing



(a)

$\left[\pm 1/2\mu \right]$



(b)

$\left[\pm 1/2\mu \right]$

Figure 1. Bright field (a), dark field (b) micrographs of γ' structure in specimen given modified commercial heat treatment. Final ageing was done at 1400°F instead of 1550°F. Note the extremely fine γ' structure that gives rise to the matrix strain contrast seen in both micrographs.

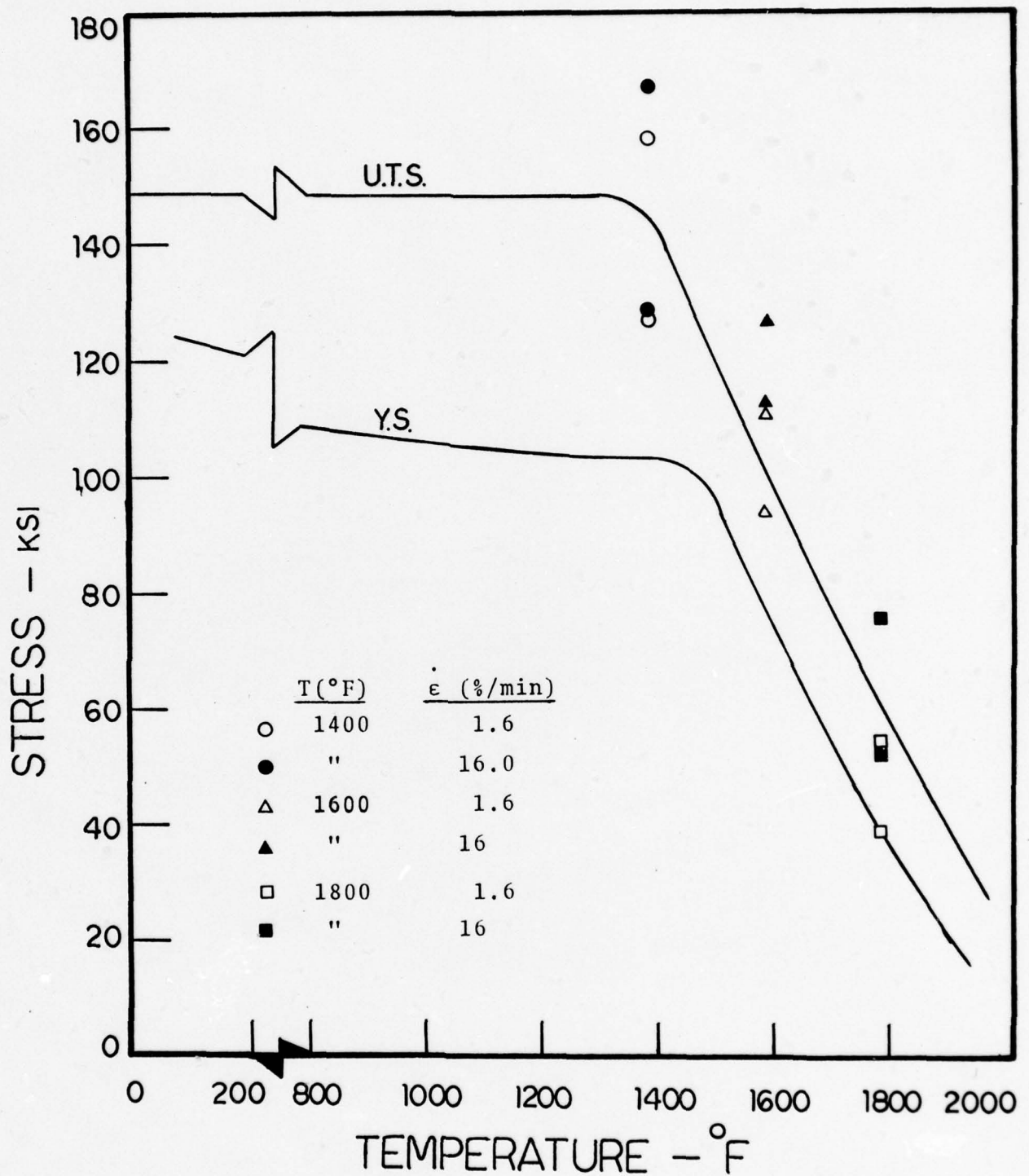


Figure 2. Tensile and yield strengths as a function of temperature. The solid lines are for material in the standard heat treat condition while the discrete data points apply to specimens whose final ageing was done at 1400°F. The strain rates are indicated in the key.

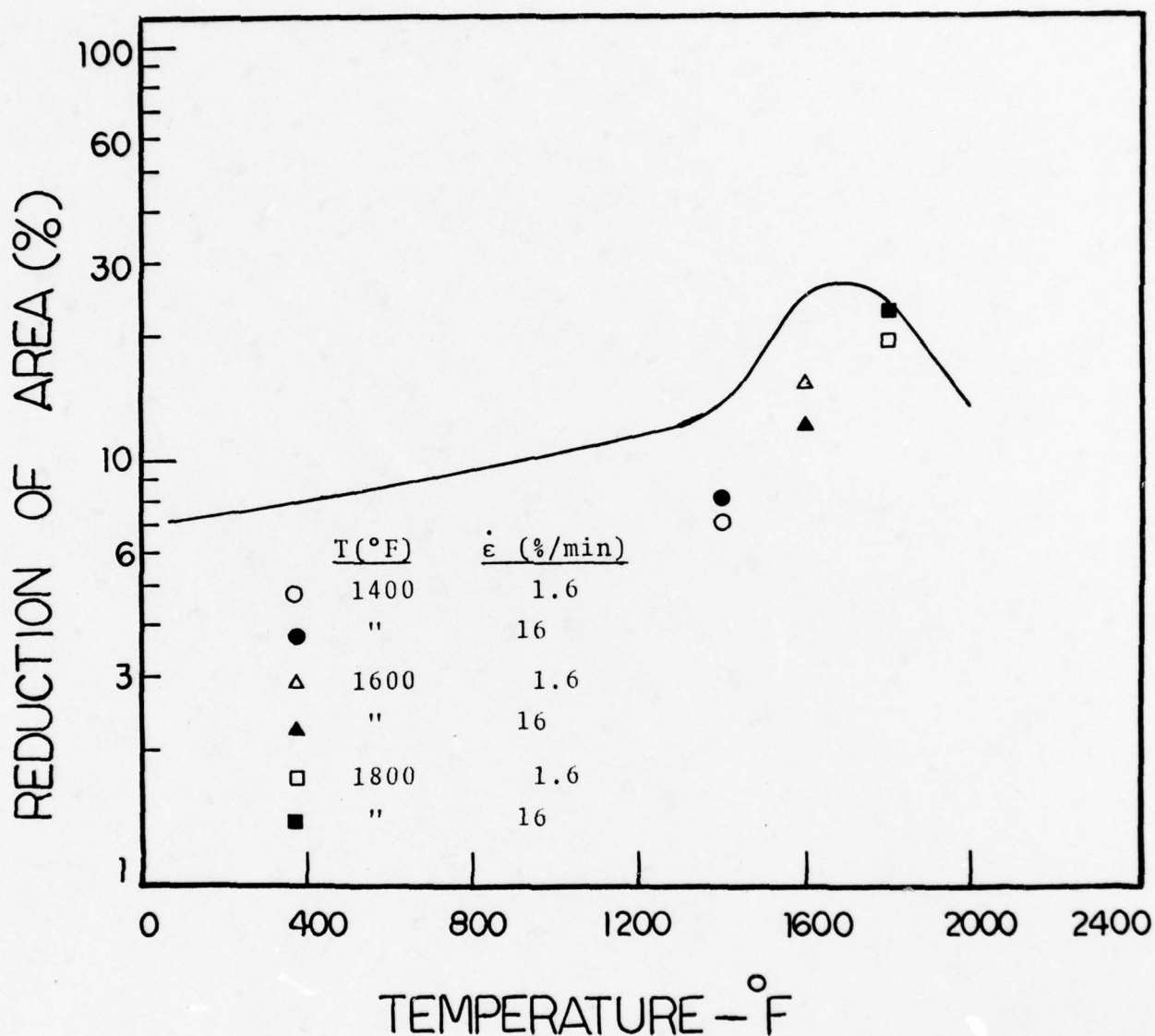


Figure 3. Ductility as a function of temperature. The solid line represents the ductility of the material in the standard heat treatment. The discrete data points apply to specimens whose final ageing temperature was 1400°F. Strain rates are indicated on the key.

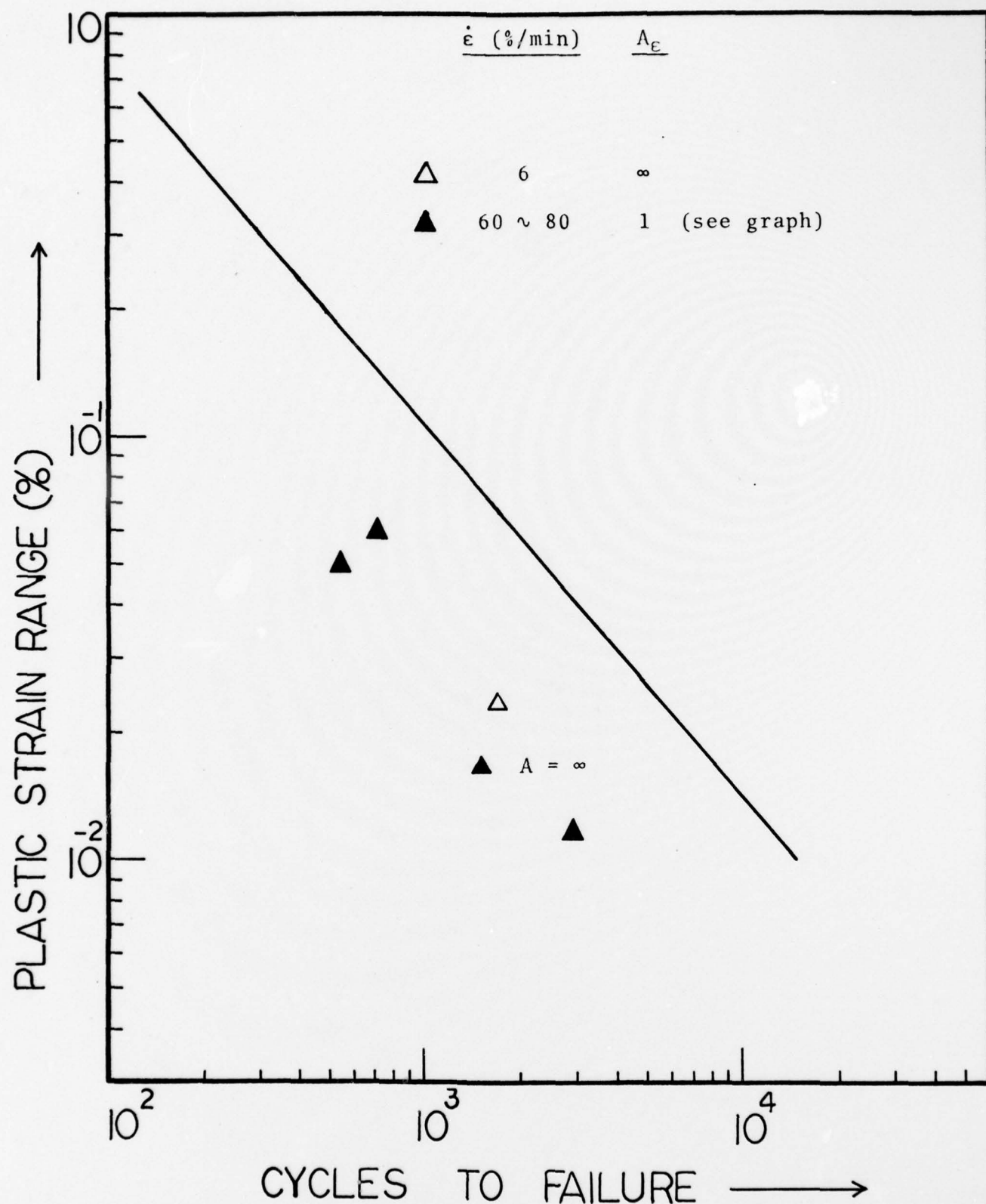


Figure 4. Coffin-Manson plot of LCF data at 1600°F. The solid line refers to the standard heat treatment. The triangles refer to material whose final ageing was at 1400°F.

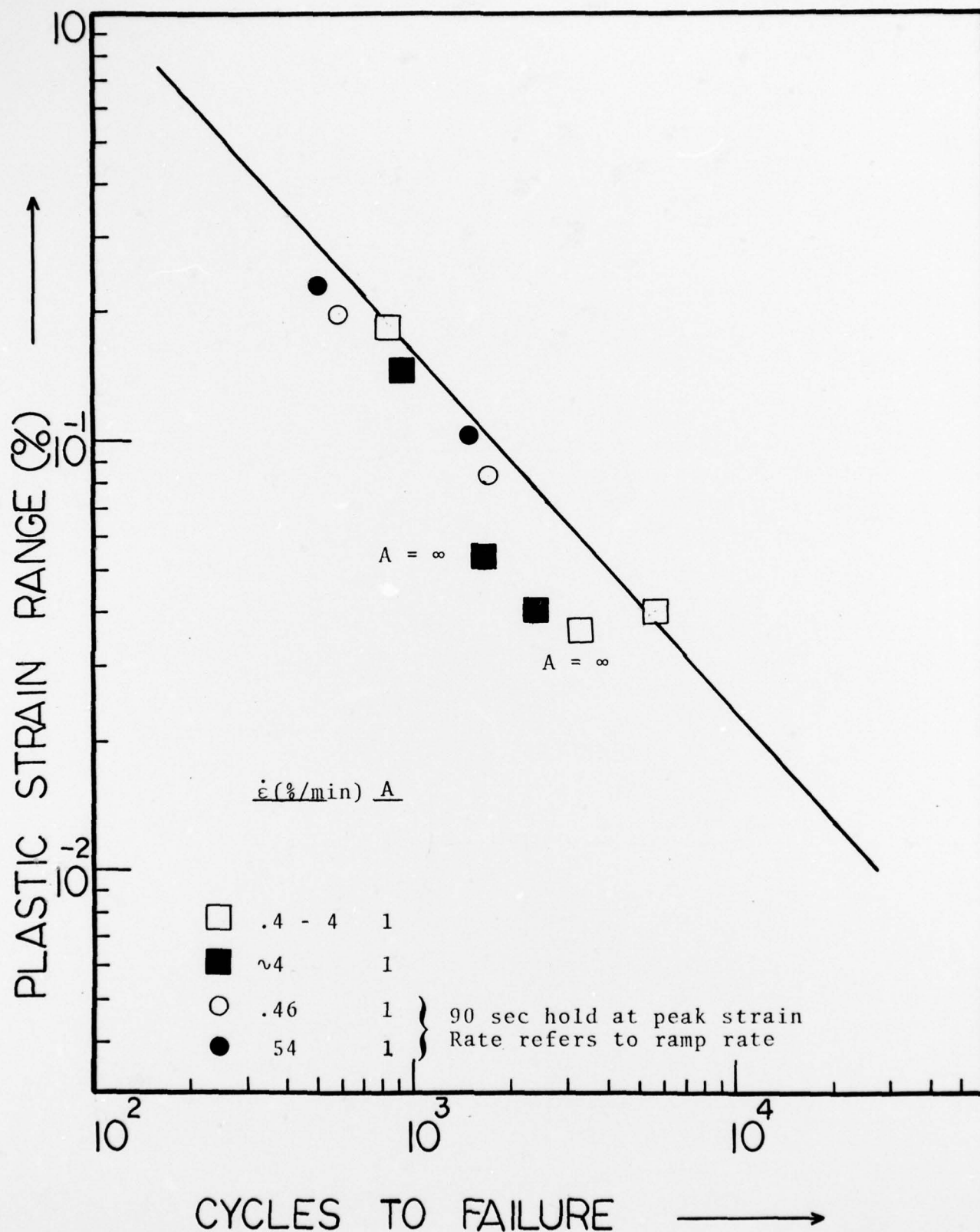


Figure 5. Coffin-Manson plot of LCF data at 1800°F. The solid line refers to the standard heat treatment. The data points refer to material whose final ageing was at 1400°F.

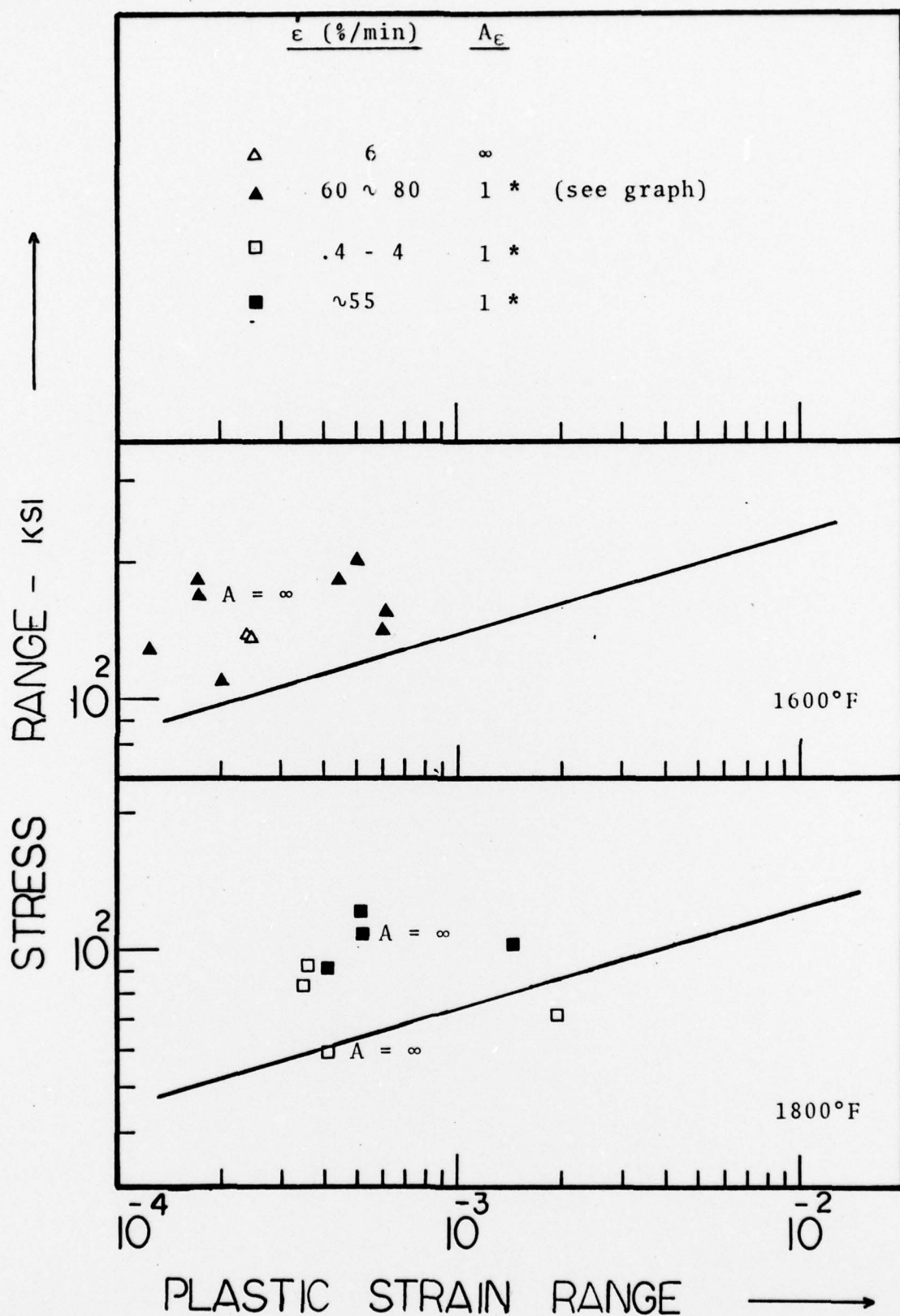
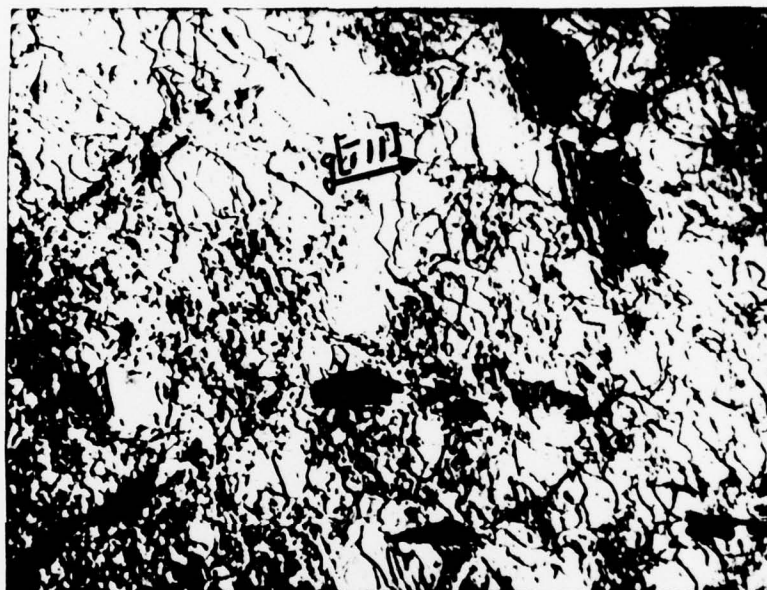


Figure 6. Cyclic stress strain curves at 1600°F and 1800°F. The solid lines refer to material in the standard heat-treat condition while other data points are shown for high and low rate tests.



| +0.5μ+ |

Fig. 7 Specimen LL-7. TEM micrograph $N_f = 1800$ $\Delta\epsilon_t = 0.7$
 $\Delta\epsilon_p = 0.006$ $v = 5$ cpm. Note the tendency to form
 linear dislocation segments in irregular arrays.
 Tested at 1400°F.

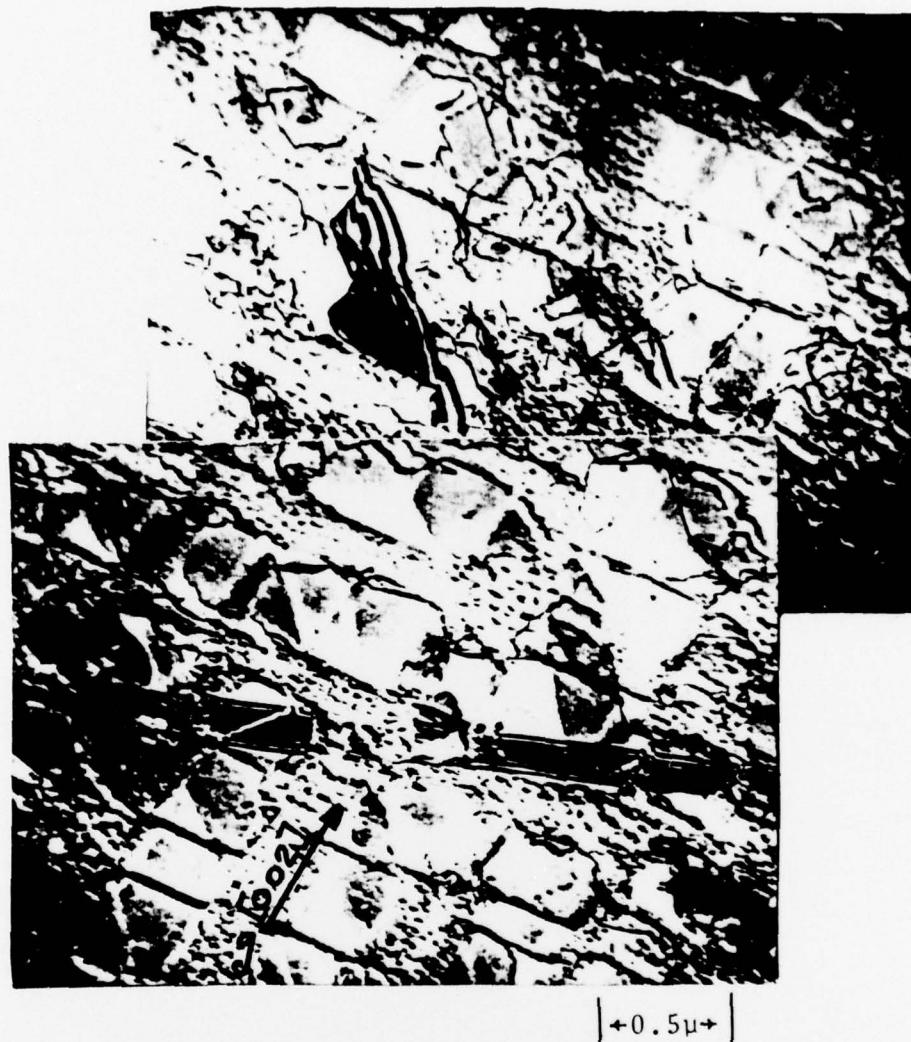
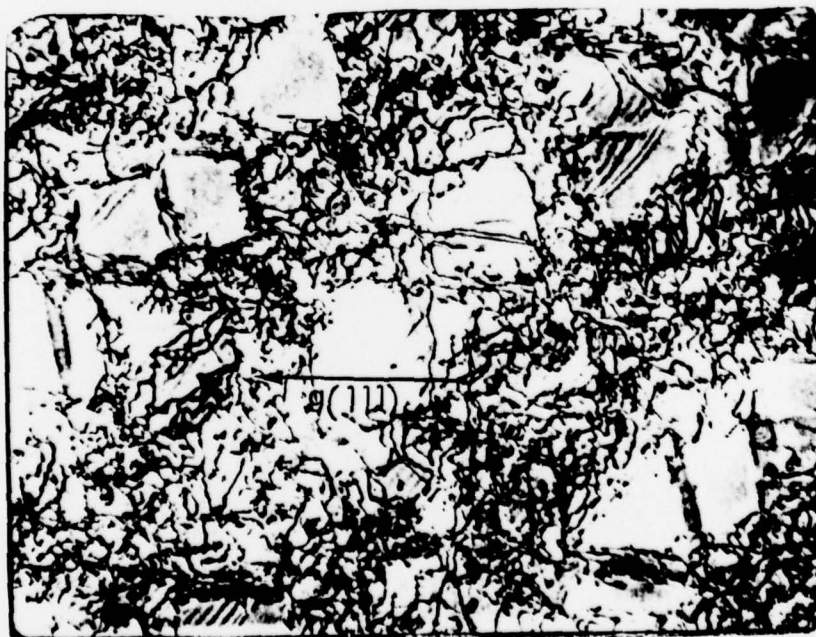


Fig. 8 Specimen LL-7. TEM micrograph $N_f = 1800$ $\Delta\epsilon_t = 0.7$
 $\Delta\epsilon_p = 0.006$ $v = 5$ cpm. Same as Fig. 7 except different
 region. Note the reduced dislocation density. 1400°F



(a)

$\{0.5\mu\}$



(b)

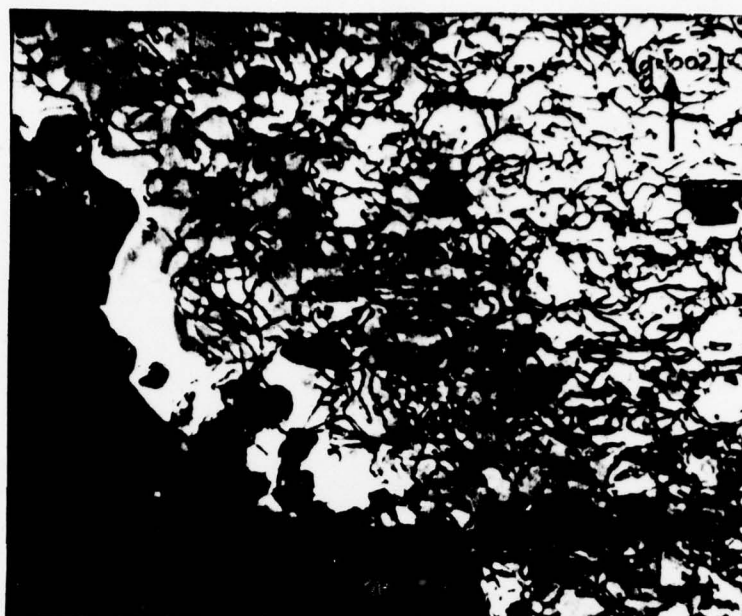
Fig. 9 LCF substructures at 1600°F. In (a), $\Delta\epsilon_p = 0.024$
 $N_f = 837$ $v = 5$ cpm. In (b), $\Delta\epsilon_p = 0.017$ $N_f = 550$
 $v = 50$ cpm.



(a)

$\left[\leftarrow 1\mu \rightarrow \right]$

Fig. 10 Specimen LL-11. $N_f = 3232$ $\Delta\epsilon_t = 0.44$ $\Delta\epsilon_p = 0.036$
 $v = 5$ cpm 1800°F. Note the regular dislocation
 arrays and the lack of residual contrast from the
 matrix indicating dissolution of the small γ' par-
 ticles.



(b)

$|+0.5\mu|$



(c)

Fig. 10 Specimen LL-12. $N_f = 1645$ $\Delta\epsilon_t = 0.59$ $\Delta\epsilon_p = 0.53$
 (cont.) $v = 50$ cpm 1800°F . In (b) $g = [002]$ and in (c) $g = [\bar{1}11]$. Note the uniform dislocation density. Note also that the arrays are less regular than in the preceeding micrograph and the dislocation damage is evidently more severe. Note also the typical boundary carbides.

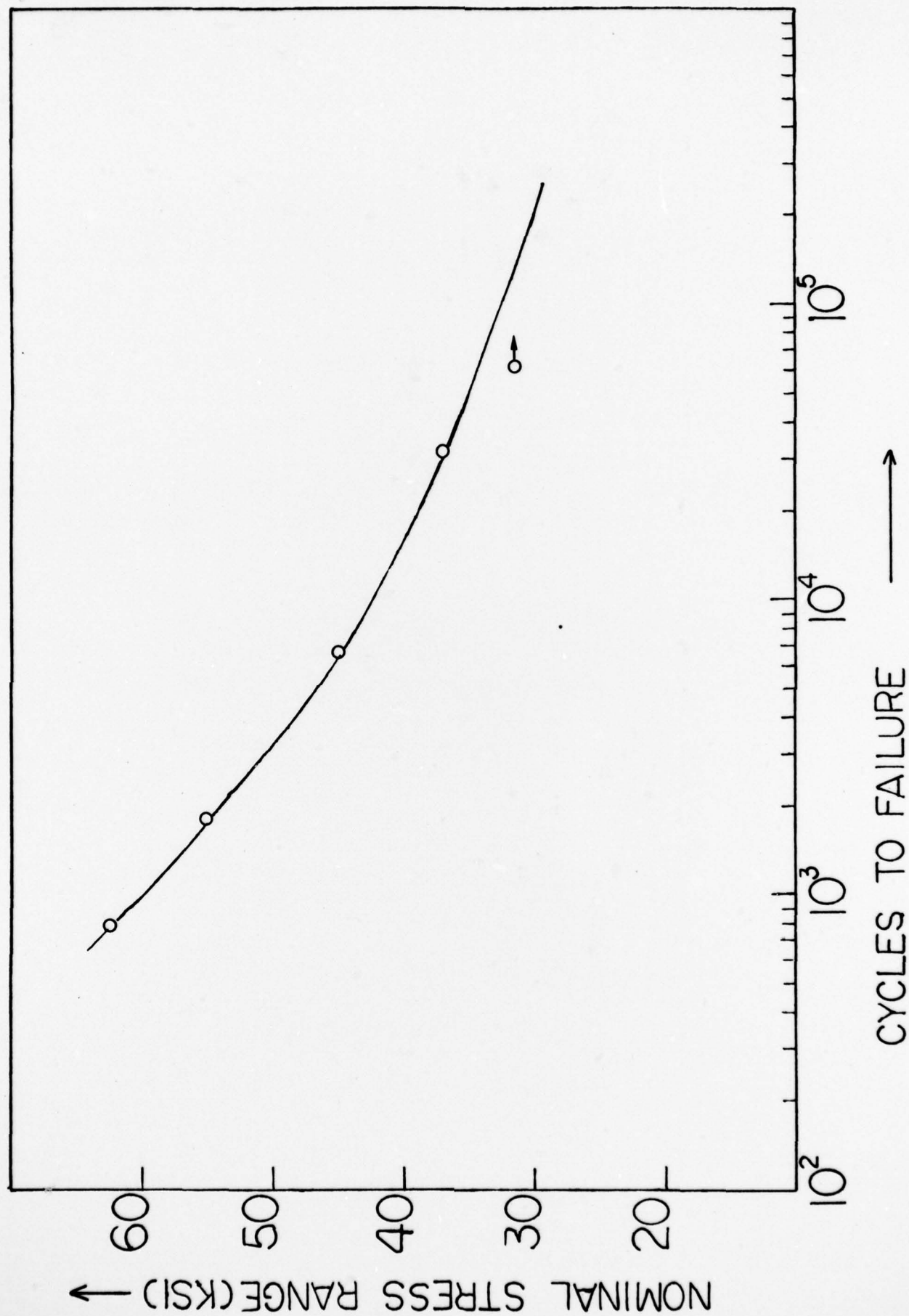


Fig. 11 Continuous cycling notch LCF test results at 1800°F.

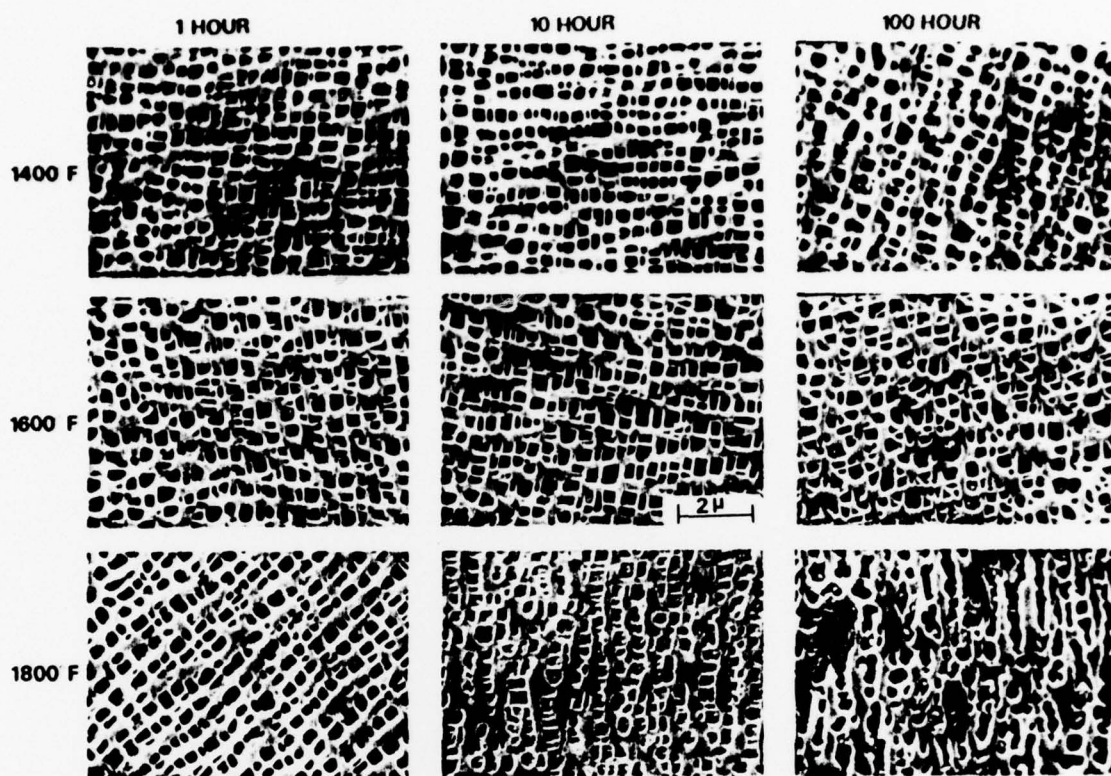


Fig. 12 Microstructural stability of heat-treated René 80 as a function of time and temperature at a stress of $1/3$ the yield stress. For the specimen exposed 100 hr. at 1800°F the γ' cubes have transformed into plates parallel to (100) matrix planes and perpendicular to the tensile axis.

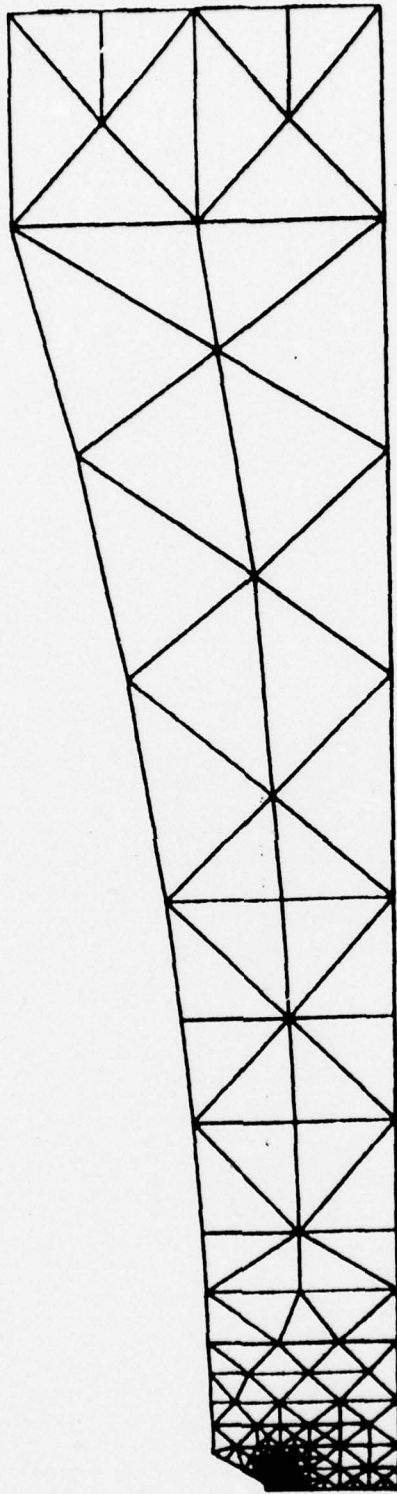


Fig. 13 Finite element model used for K_t determination.

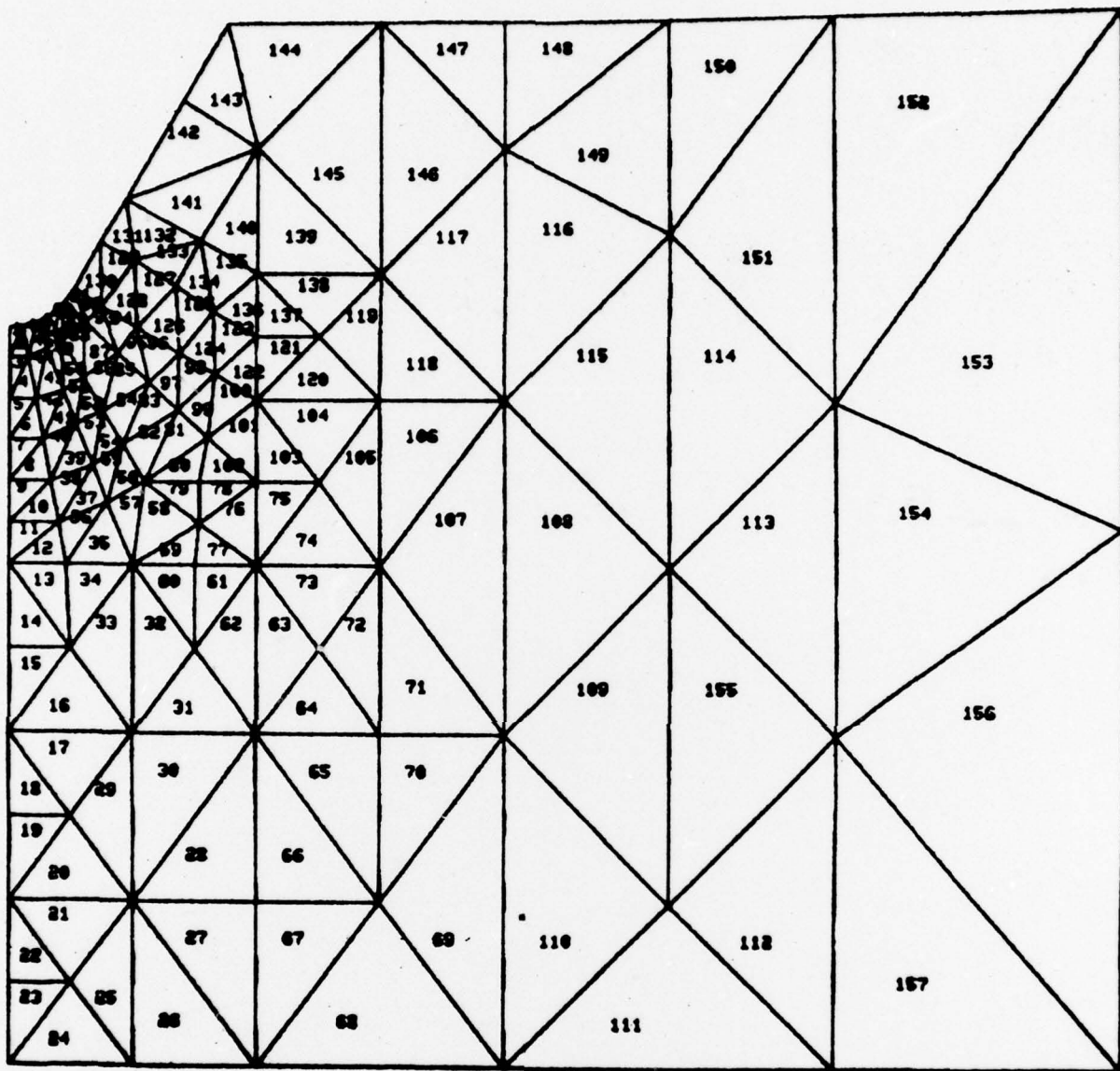
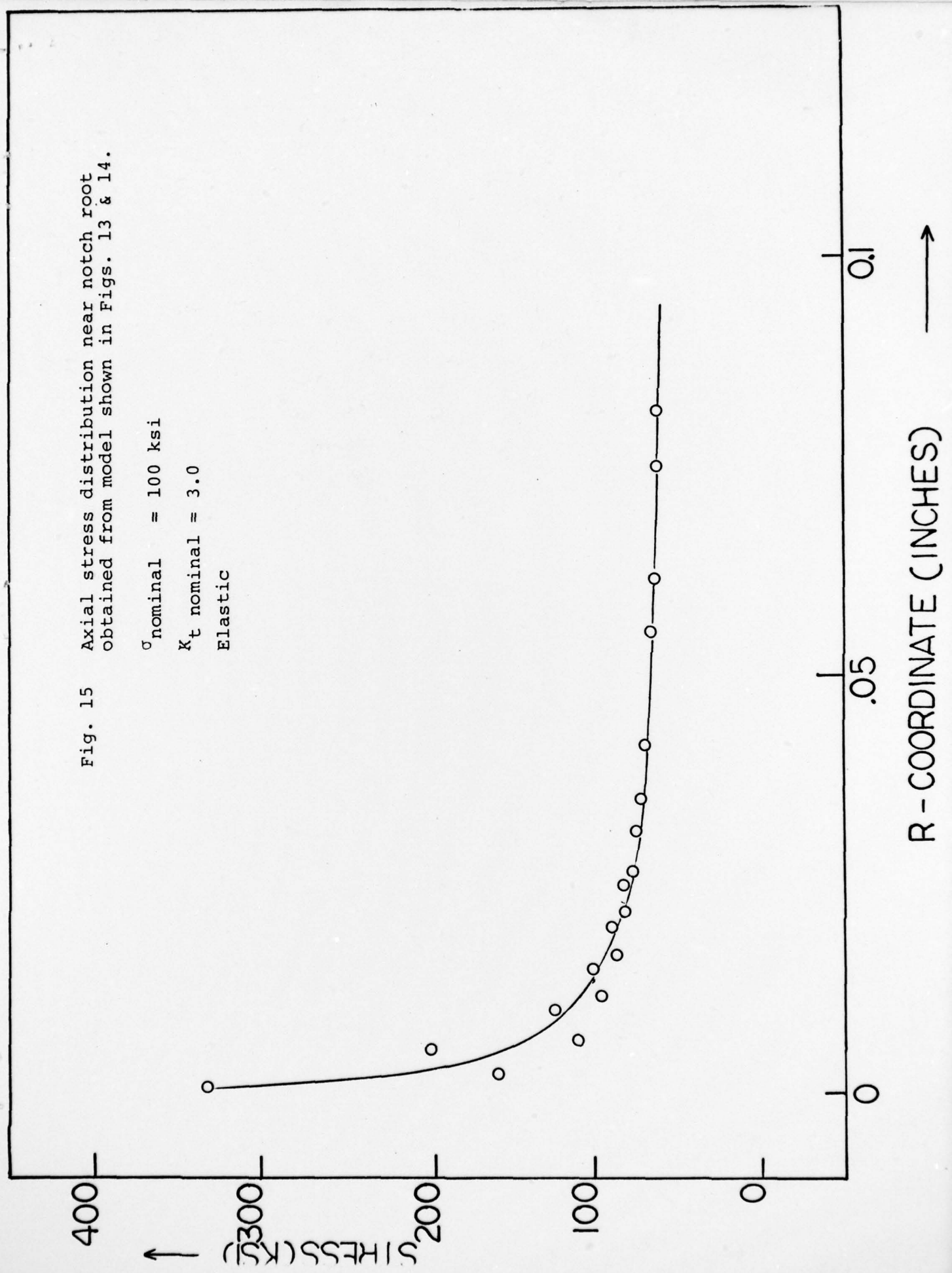


Fig. 14 Enlarged region near notch of finite element model in Fig. 13. (Numbers are element numbers).

Fig. 15 Axial stress distribution near notch root
obtained from model shown in Figs. 13 & 14.

$\sigma_{\text{nominal}} = 100 \text{ ksi}$
 $K_t \text{ nominal} = 3.0$
Elastic



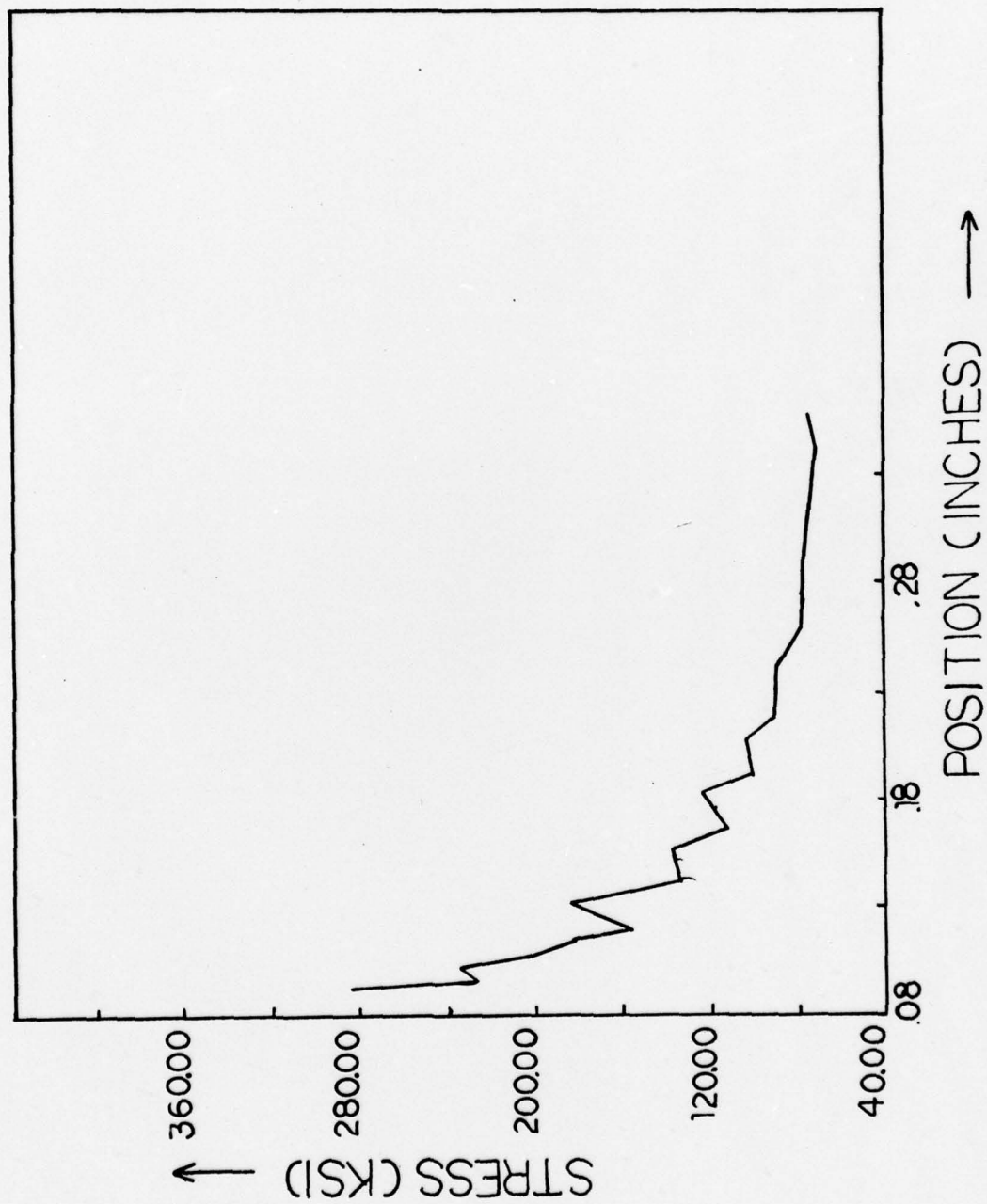


Fig. 16 Axial stress near notch root. Predicted K_t is 3.30.

IED
78